Assessment of hydrogen embrittlement via image-based techniques in Al-Zn-Mg-Cu aluminum alloys

Su, Hang
Department of Mechanical Engineering, Kyushu University

Toda, Hiroyuki
Department of Mechanical Engineering, Kyushu University

Shimizu, Kazuyuki
Department of Mechanical Engineering, Kyushu University

Uesugi, kentaro
Japan Synchrotron Radiation Research Institute(JASRI)

他

出版情報：Acta Materialia. 176 (1), pp.96-108, 2019-09-01. Elsevier
バージョン：
権利関係：

Figures and tables

Table.1 Chemical compositions of the three alloys (mass %)

	Si	Fe	Cu	Mg	Zn	Ti	Zr	Al
High Fe Si	0.30	0.30	1.50	2.40	10.00	0.04	0.15	Bal
Low Fe Si	0.01	0.01	1.50	2.40	10.00	0.04	0.15	Bal

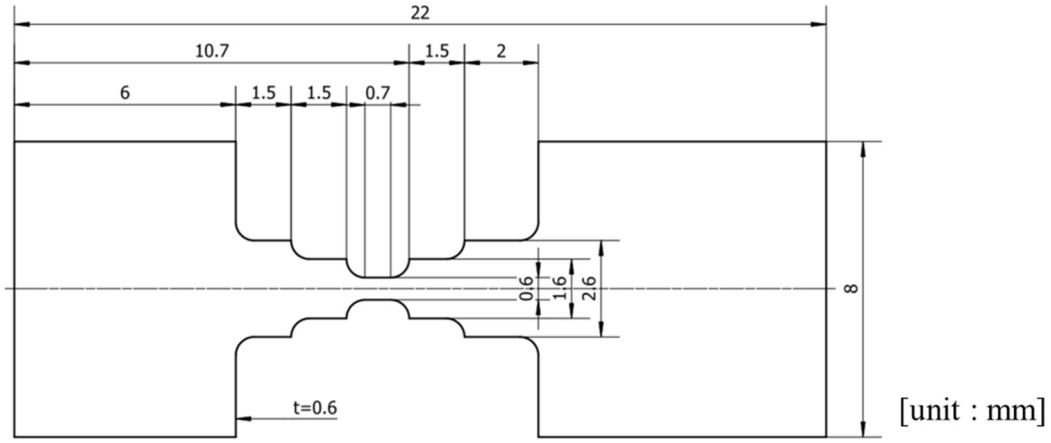

Fig.1 Geometry of an in-situ tensile test specimen

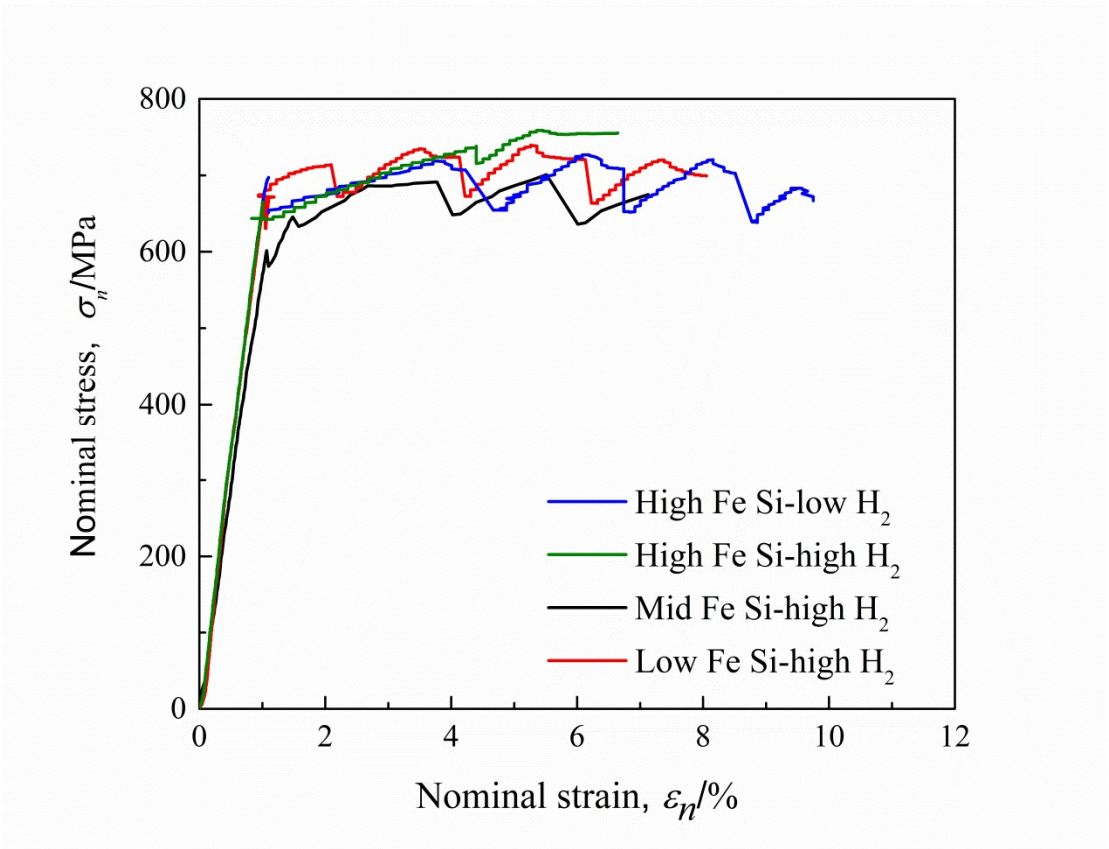

Fig. 2 Nominal stress-strain curves for the in-situ tensile tests. It is worth noting that nominal stress-strain curve of Mid Fe Si-high H_2 has already been applied in Ref [15].

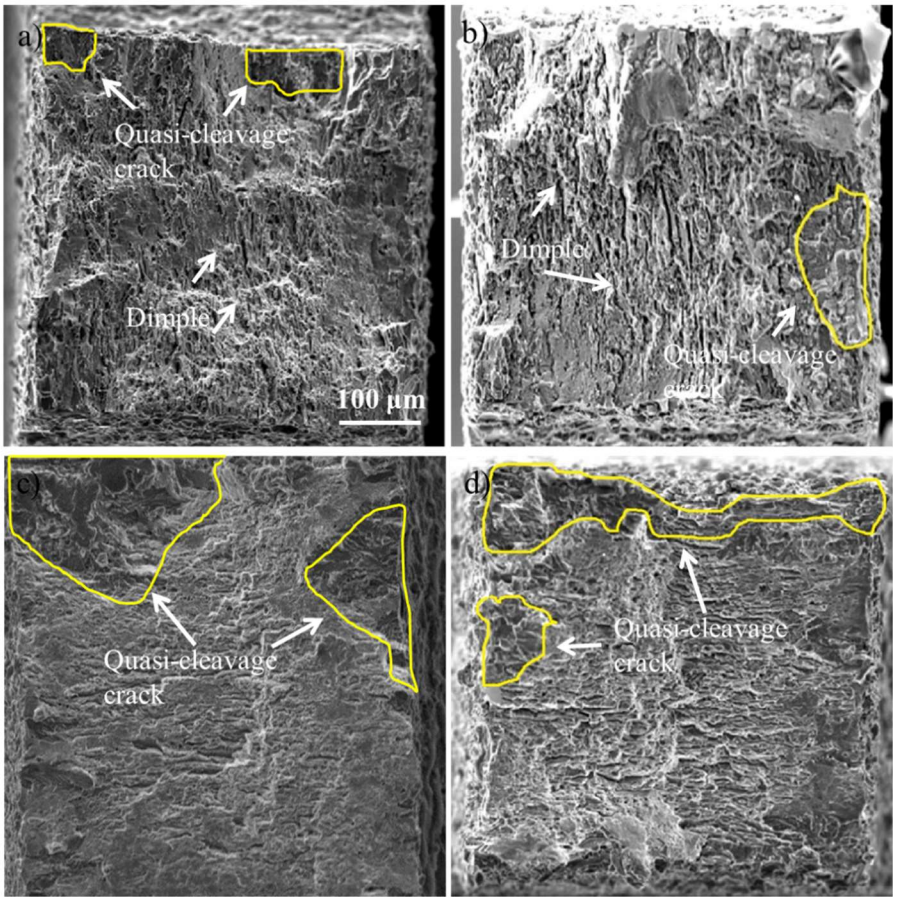

Fig.3 Fracture surfaces after the in-situ tensile tests; a) High Fe Si-low H_2 specimen, b) High Fe Si-high H_2 specimen, c) Mid Fe Si-high H_2 specimen [15] and d) Low Fe Si-high H_2 specimen; the quasi-cleavage crack region is identified by yellow solid lines.

Table.2 Areal fractions of the quasi-cleavage cracks

Materials	Areal fraction [%]
High Fe Si-low H_2	5.7
High Fe Si-high H_2	8.1
Mid Fe Si-high H_2	18.8 [15]
Low Fe Si-high H_2	22.4

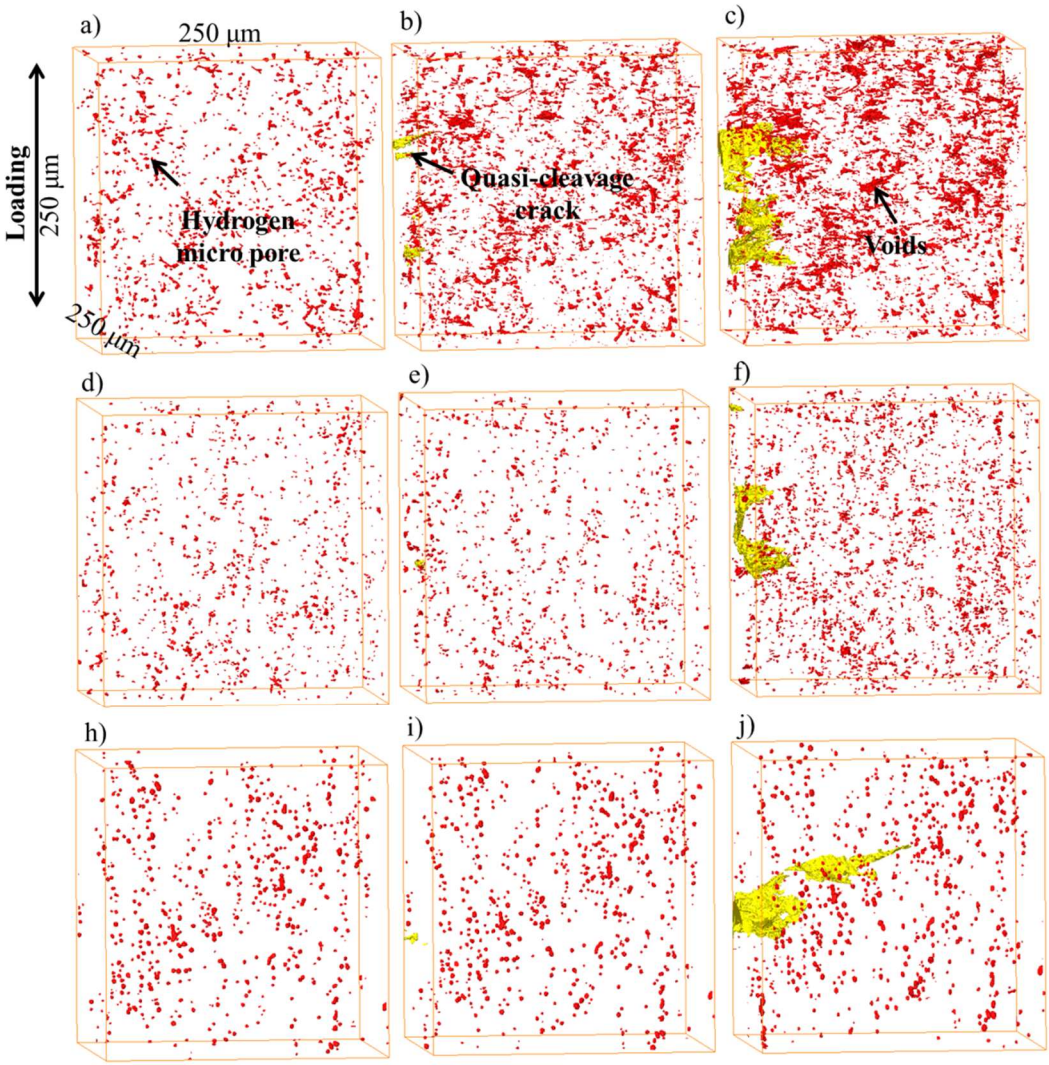

Fig.4 4D observations of the initiation and propagation of the quasi-cleavage crack in High Fe Si-low H_2 under different applied strains; a) ε_a = 0.0 %, b) ε_a = 6.3 % and c) ε_a = 8.6 %; in High Fe Si-high H_2 under different applied strains; d) ε_a = 0.0 %, e) ε_a = 1.0 % and f) ε_a = 4.4 % and that in Low Fe Si-high H_2 under different applied strains; h) ε_a = 0.0 %, i) ε_a = 2.4 % and j) ε_a = 6.9 % Hydrogen micro pores are shown in red and the quasi-cleavage crack is shown in yellow

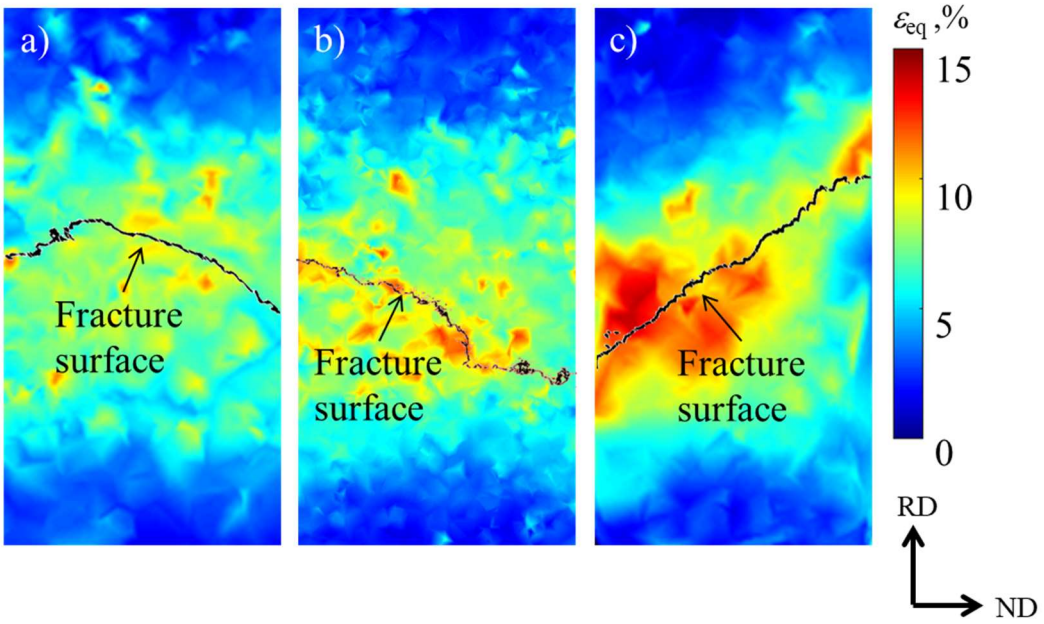

Fig. 5 The equivalent strain (ε_{eq}) distribution under different applied strains, viewed on the y-z (RD-ND) cross-section; a) equivalent strain map calculated between ε_a of 2.1 and 6.3 % in High Fe Si-low H_2, b) equivalent strain map calculated between ε_a of 0 and 4.4 % in High Fe Si-high H_2 and c) equivalent strain map calculated between ε_a of 2.4 and 6.9 % in Low Fe Si-high H_2. Fracture surface is shown as the black line.

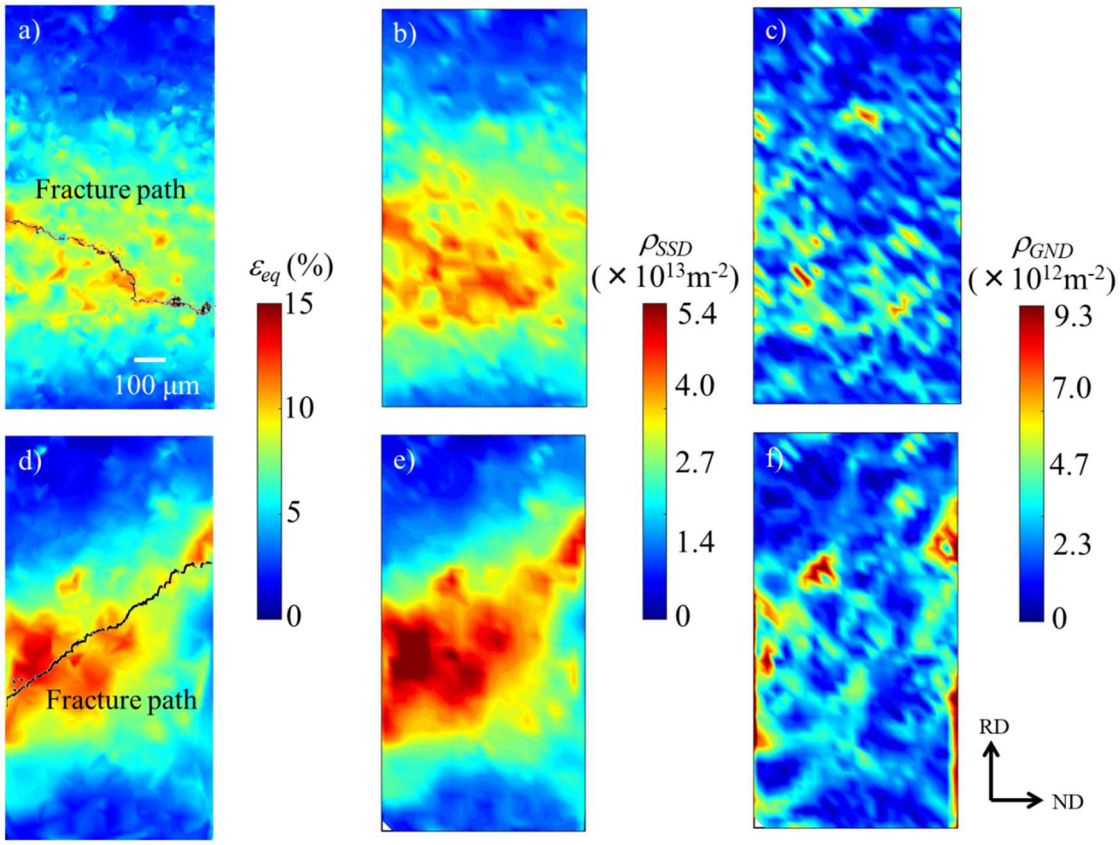

Fig. 6 SSD and GND densities calculated from the equivalent strain (ε_{eq}) mapping under different applied strains, viewed on the y-z (RD-ND) cross-section; a) equivalent strain map calculated between ε_a of 2.1 and 6.3 % in High Fe Si-high H_2, b) SSD density calculated from a), c) GND density calculated from a); d) equivalent strain map calculated between ε_a of 2.4 and 6.9 % in Low Fe Si-high H_2, e) SSD density calculated from d) and f) GND density calculated from d). Fracture path is shown as the black line in a) and d).

Table. 3 Binding energy of each hydrogen trap site in Al-Zn-Mg-Cu aluminum alloys

Trap Site	Binding energy E_b/KJmol^{-1}	Trap Site	Binding energy E_b/KJmol^{-1}
Edge dislocation	9.64[25]	Precipitates	33.77[26]
Screw dislocation	7.72[25]	Intermetallic particles	28.10[43]
Vacancy	28.95[24]	Pore	67.20[44]
Grain boundary	19.30[24]		

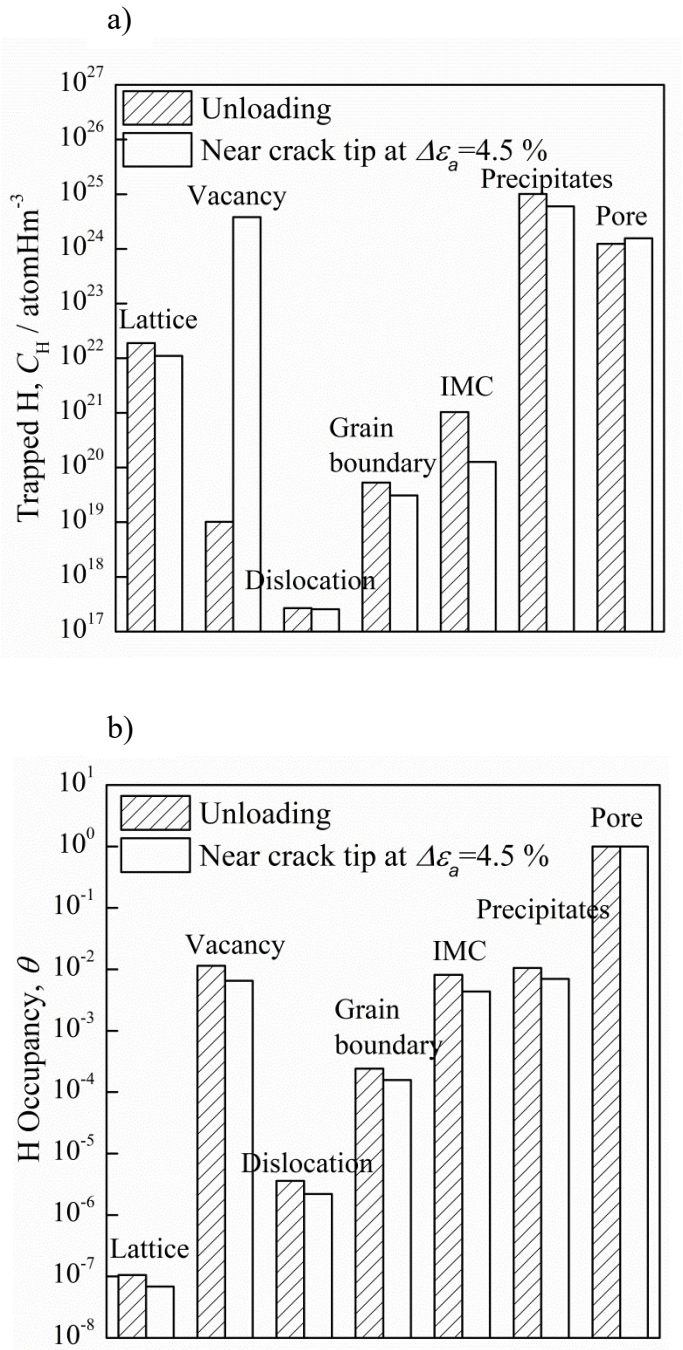

Fig. 7 Comparisons of the hydrogen trapping behavior between the whole specimen at unloading state and a region ahead of the hydrogen-induced quasi-cleavage crack tip an applied strain of 4.5 % in Low Fe Si-high H_2 specimen; a) trapped hydrogen content and b) hydrogen trapping occupancy

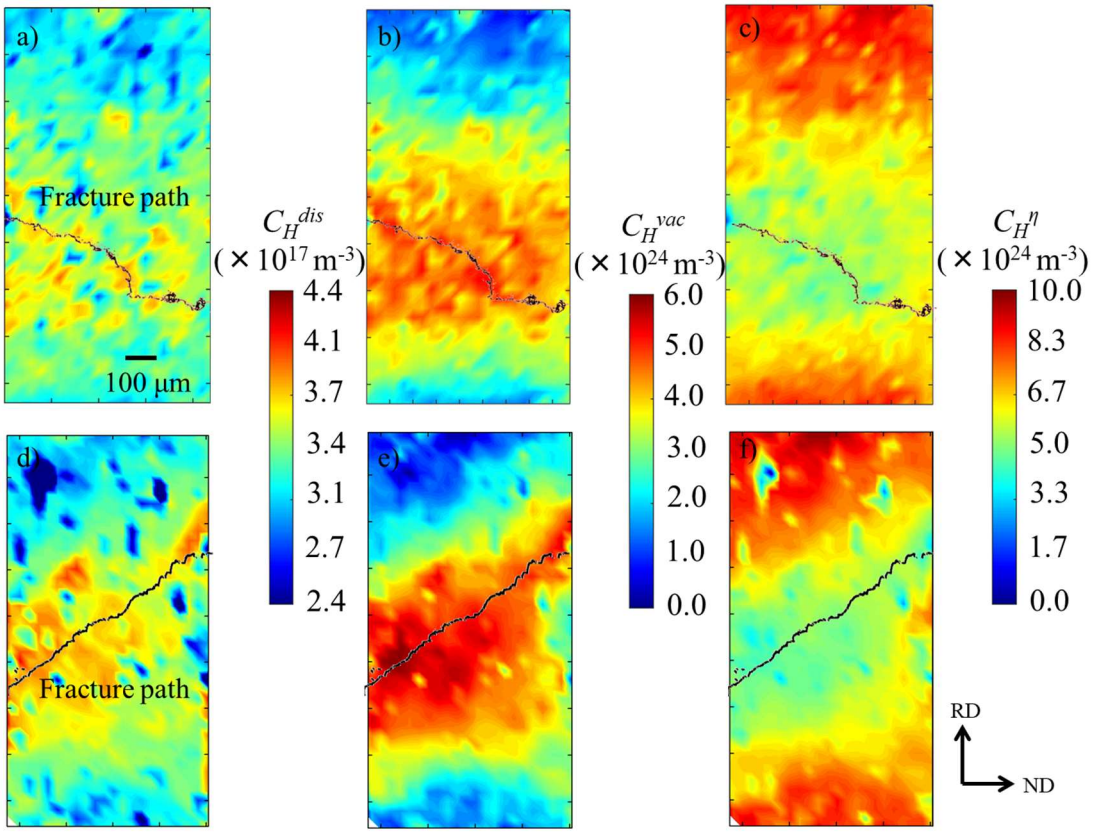

Fig. 8 Hydrogen concentrations at various trap sites including dislocations, vacancies and precipitates that calculated from the equivalent strain (ε_{eq}) mapping at an applied strain, $\triangle\varepsilon_a$ of approximately 4.5 %, viewed on the y-z (RD-ND) cross-section; a) and d) is the hydrogen concentration at dislocations in High Fe Si-high H_2 and Low Fe Si-high H_2 specimen, b) and e) is the hydrogen concentration at vacancies in High Fe Si-high H_2 and Low Fe Si-high H_2 specimen and c) and f) is the hydrogen concentration at precipitates in High Fe Si-high H_2 and Low Fe Si-high H_2 specimen. Fracture surface is shown as the black line.

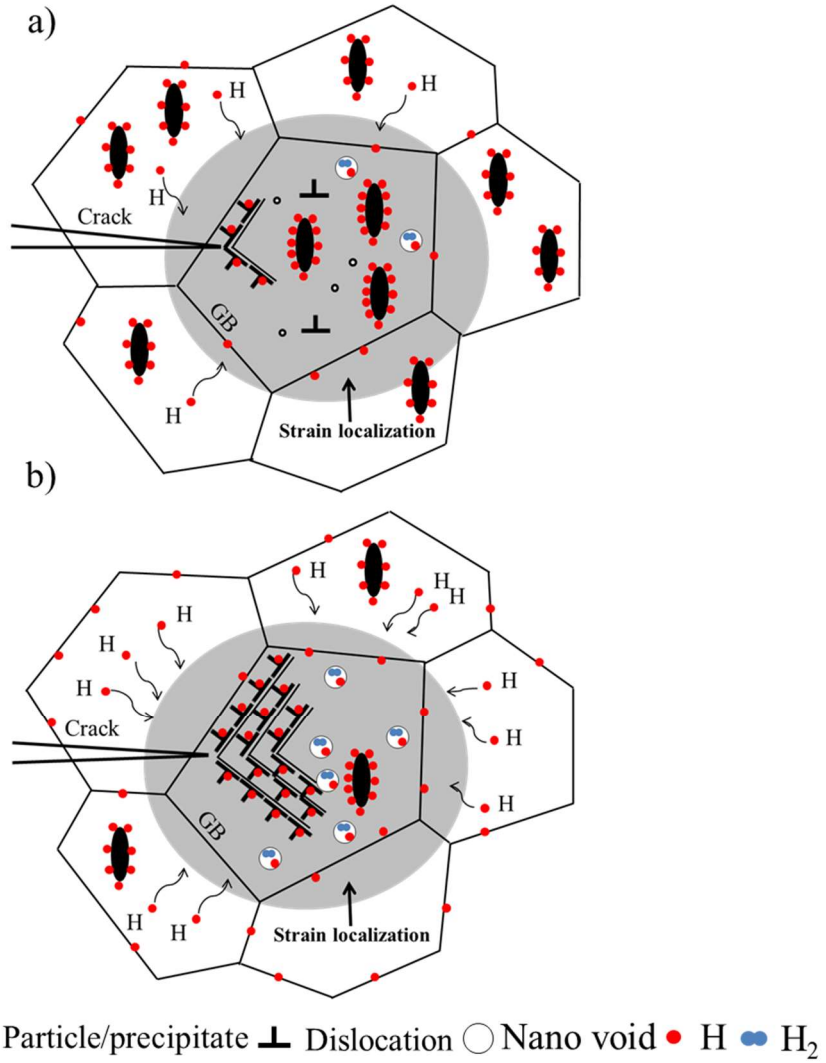

Fig.9 Schematic illustration of the influence of intermetallic particles to the hydrogen partitioning and related crack propagation in the strain localization region, a) high intermetallic particle content material and b) low intermetallic particle content material